Asian Journal of Scientific Research

ISSN 1992-1454

science alert
http://www.scialert.net

ANSInet
an open access publisher
http://ansinet.com

Asian Journal of Scientific Research 1 (3): 213-221, 2008
ISSN 1992-1454

Computation of the Scattering Parameters Using Indian Lognormal Drop Size Distribution at 16, 19.3 and 34.8 GHz for Spherical and Oblate Spheroidal Rain Models

Aderemi Sikiru Adekola
Department of Physics, Federal University of Technology, Akure, Nigeria

Abstract: Calculations of Millimeter-wave rain scattering parameters are made at 16, 19.3 and 34.8 using spherical and oblate spheroidal rain models. Computations are made at angle of incidence of 0 and 90° for the oblate spheroidal rain model. The characteristic of the difference between the two models with rain rate are studied at incidence angle of 0° to allow us determine their suitability in a tropical environment. Some propagation parameters are evaluated using the Indian lognormal and Marshall and Palmer (MP) Drop Size Distributions (DSD's). Marshall and Palmer DSD model could underestimate rain-induced attenuation at all the frequencies in the rain rate range of $0.25 \leq R < 50$ mm h^{-1} and overestimate specific phase shift at rain rate $R > 100$ mm h^{-1} if adopted for radio wave propagation prediction on tropical path. However, Indian data compare well with MP at rain rate in the range $50 \leq R \leq 100$ mm h^{-1}. Similarly, spherical rain model could underestimate the specific attenuation with a maximum margin of 3.4 dB km^{-1} at 34.8 GHz and specific phase shift of 15.7° km^{-1} at 16 GHz, both at rain rate of 150 mm h^{-1}. The empirical scaling relationship between the radar reflectivity η and rain rate R ($\eta = aR^b$) are derived for the Indian DSD and the coefficients a and b compare well with those of Aydin and Lure.

Key words: Oblate spheroidal raindrops, spherical rain model, specific attenuation, specific phase shift, drop size distribution, rain rate, scattering

INTRODUCTION

It is well recognized that rain is the major factor that adversely affect the propagation of electromagnetic wave signals especially at frequencies above 10 GHz. The knowledge of its scattering characteristics in a location of interest is therefore very crucial in the engineering of reliable communication system. Scattering properties of oblate spheroidal at both horizontal and vertical polarizations are very important in the estimation of crosstalk. The feasibility of using orthogonal polarizations to increase channel capacity in both satellite and terrestrial systems depends on the cross polarization isolation that is obtainable under worst-case system operating conditions (Oguchi, 1980).

There have been significant contributions to the study of interaction between raindrop and the incident electromagnetic waves using temperate data (for a partial list, see references cite in Ognchi, 1980, 1986, 1991). However, a few authors (Ajayi and Ofuche, 1984; Ajewole *et al*., 1999) have investigated the study of interaction of radio signals with tropical rain data, which had contributed to the reason for dearth rain-induced impairments data for the tropics especially over Indian continent (Kunhikrishnan *et al*., 2006). Verma and Jha (1996) had earlier reported the Indian lognormal Drop Size Distribution (DSD) and comparison was made with those of Nigeria and Brazil.

This paper reports the result obtained from the computation of the scattering parameters using Indian lognormal drop size distribution of Verma and Jha (1996) at frequencies of 16, 19.3 and 34.8 GHz for spherical and oblate spheroidal rain models. The computations are performed with the Mie theory technique for the spherical rain model while empirical relation counecting the attenuation

and phase shift with propagation constant of Oguchi (1983) was employed for the oblate spheroidal rain model. The spherical raindrops assumed temperature of 20° and their refractive index and propagation constant at this temperature are calculated at the chosen frequencies using the model reported in Ray (1972). The characteristics of rain-induced impairments with spherical rain model do not depend on the polarization of the incident wave or on the angle of incidence while calculations using oblate spheroidal rain model are performed at angle of incidence of 0 and 90° to the surface of the raindrop. The scattering parameters at incidence angle of 0° are the same for horizontal and vertical polarizations with oblate spheroidal rain model. On this basis, the results with spherical and oblate spheroidal rain models are compared at incidence angle of 0°. The frequency characteristics of the differential attenuation and differential phase shift for the two orthogonal linear polarizations are investigated. Radar reflectivity for spherical rain model and its variation with rain rate and frequency are studied. The coefficients of the power law relationship between the radar reflectivity and rain rate are derived and this have direct dependence on the drop size distribution employed which invariably reflects the influence of climatic on the electromagnetic waves as it propagates.

COMPUTATIONAL PROCEDURE OF THE SCATTERING PARAMETERS

The scattering computations were performed using the generalized lognormal drop size distributions of the form

$$N(D) = \frac{N_T}{\sigma D\sqrt{2\pi}} \exp\left[-\frac{1}{2}\left(\frac{\ln(D)-\mu}{\sigma}\right)^2\right] \quad (m^{-3}\,mm^{-1}) \tag{1}$$

It represents the number of drops, N, of diameter D in unit volume, it follows therefore that N(D) is the number of drops per unit volume per diameter interval, μ is the mean of ln (D), σ is the standard deviation and N_T is the number of drops of all sizes. The parameter of the lognormal; μ, σ and N_T for the Indian region credited to Verma and Jha (1996) is:

$$\begin{aligned} N_T &= 169.05R^{0.2937} \\ \mu &= -0.05556 + 0.130961\ \text{InR} \\ \sigma^2 &= 0.30042 - 0.023604\ \text{InR} \end{aligned} \tag{2}$$

The correlation coefficient is better than 0.95 and standard error of correlation coefficient is less than 0.0015. The raindrop size distribution are calculated for 13 equivolume raindrops with radii in the range 0.25-3.25 mm at rain rates varying from 0.25-150 mm h^{-1}.

The backscattering cross section Q^B integrated over the drop size distribution N (D) leads to the radar reflectivity (Aydin and Lure, 1991) which is express as:

$$\eta = \int_0^{D_{max}} Q_B(D)N(D)dD \quad (mm^{-2}\ m^{-3}) \tag{3}$$

Q_B is defined as the backscattering cross section, it is express as:

$$Q_B = \frac{1}{q^2}\left|\sum_{n=1}^{\infty}(2n+1)(-1)^n(a_n + b_n)\right|^2 \tag{4}$$

The nth electric partial wave has amplitude a_n and b_n is the magnitude of the nth magnetic partial wave and $q = k_0a = 2\pi na/\lambda$. Basic equations relevant in the computation of scattering parameters using Mie theory has been reported in Adekola (2002). Calculations of radar reflectivity are performed for spherical rain model at all the frequencies considered in this study and the power law relation between the radar reflectivity and rain rate are derived.

The Attenuation, A in dB and the Phase shift, Φ in degrees for two characteristics polarizations are given by Oguchi (1981).

$$A_{H,V} = 8.686 \text{ Im } (k_{H,V}L) \tag{5}$$

$$\Phi_{H,V} = \frac{180}{\pi} \Re (k_{H,V}L) \tag{6}$$

Where:

L = The propagation path length,
$k_{H,V}$ = The propagation constant.

Assuming that plane waves with electric fields polarized in the horizontal and vertical directions are incident on the rain medium, Oguchi (1966) earlier proposed an expression for the propagation constant given as:

$$k_{H,V} = \frac{2\pi}{k_0} \int_0^\infty f_{H,V}(0)\, N(D)\, dD \tag{7}$$

Where:

$f_{H,V}(0)$ = The scattering amplitude functions of a raindrop with diameter D in the forward direction and for horizontal and vertical polarizations,
k_0 = The free-space wave number.

Calculation of attenuation and phase shift are done at propagation path length of 1 km.

RESULTS AND DISCUSSION

The calculations are performed for spherical and oblate spheroidal rain models at 16, 19.3 and 34.8 GHz frequencies and at rain rate between 0.25 and 150 mm h^{-1} based on scattering by single particle and based on tropical lognormal drop size distribution of India region. The chosen frequencies are of practical importance to terrestrial and earth-satellite communication systems. The results of the calculation for spherical rain model do not depend on the polarization of the incident wave or on the angle of incidence while calculations using oblate spheroidal rain model are performed at angle of incidence of 0 and 90° to the surface of the raindrop. Also note that the scattering parameters at incidence angle of 0° are the same for horizontal and vertical polarizations. This gives an avenue for comparison between the results using spherical and oblate spheroidal rain models since there is no difference between horizontal and vertical polarized scattering parameters when spherical rain model is assumed.

The results of specific attenuation and specific phase shift are shown in Table 1 for spherical rain model at 16, 19.3 and 34.8 frequencies and Table 2-4 for oblate spheroidal rain model at 16, 19.3 and 34.8 GHz, respectively. The specific attenuation and specific phase shift in both polarizations becomes very large as the rain rate increase and as frequency also increases. This is an indication that increase in the frequency of the radio signal propagated through rain medium will deteriorate the quality of the signal at the receiver end. High rain rate will also adversely affect the radio signal in the same

Table 1: Specific attenuation and specific phase shift using spherical rain model based on tropical lognormal drop size distribution and comparison with Marshall and palmer

	Specific attenuation (dB km^{-1})						Specific phase shift (Deg km^{-1})					
	16 GHz		19.3 GHz		34.8 GHz		16 GHz		19.3 GHz		34.8 GHz	
RR	India	MP	India	MP	India	MP	India	MP	India	MP	India	MP
0.25	0.203	0.008	0.280	0.013	0.662	0.054	3.377	0.797	3.826	0.966	4.815	1.737
1.25	0.563	0.054	0.769	0.086	1.738	0.319	8.377	3.163	9.391	3.807	11.062	6.578
2.5	0.872	0.123	1.186	0.193	2.626	0.674	12.368	5.680	13.793	6.797	15.722	11.385
5	1.351	0.279	1.829	0.425	3.960	1.393	18.237	10.143	20.227	12.043	22.239	19.355
12.5	2.406	0.802	3.237	1.175	6.788	3.492	30.404	21.561	33.455	25.285	34.870	37.760
20	3.233	1.353	4.335	1.948	8.934	5.481	39.474	31.531	43.246	36.704	43.729	52.326
25	3.719	1.727	4.979	2.468	10.173	6.755	44.670	37.699	48.834	43.716	48.635	60.837
50	5.740	3.619	7.649	5.062	15.197	12.655	65.512	65.137	71.118	74.507	67.328	95.438
75	7.396	5.506	9.828	7.612	19.188	17.998	81.889	89.128	88.508	100.985	81.125	122.635
100	8.850	7.370	11.739	10.107	22.624	22.954	95.898	110.984	103.314	124.807	92.423	145.682
125	10.170	9.206	13.470	12.548	25.695	27.612	108.370	131.305	116.447	146.733	102.144	165.965
150	11.393	11.013	15.072	14.937	28.502	32.032	119.738	150.434	128.381	167.196	110.756	184.233

MP: Marshall and Palmer; RR: Rain rate in mm h^{-1}

Table 2: Specific attenuation and specific phase shift of vertically and horizontally polarized wave at frequency of 16 GHz for 1 km propagation path based on tropical lognormal drop size distribution and comparison with Marshall and palmer

	Specific attenuation (dB km^{-1})						Specific phase shift (Deg km^{-1})					
	India			MP			India			MP		
	$\alpha = 90°$			$\alpha = 90°$			$\alpha = 90°$			$\alpha = 90°$		
RR	H	V	$\alpha = 0°$	H	V	$\alpha = 0°$	H	V	$\alpha = 0°$	H	V	$\alpha = 0°$
0.25	0.225	0.178	0.222	0.009	0.008	0.008	3.485	3.137	3.612	0.800	0.790	0.800
1.25	0.628	0.491	0.622	0.055	0.052	0.054	8.678	7.708	9.058	3.185	3.106	3.187
2.5	0.977	0.758	0.969	0.127	0.118	0.123	12.835	11.329	13.442	5.737	5.546	5.750
5	1.518	1.170	1.508	0.290	0.265	0.279	18.960	16.622	19.931	10.285	9.833	10.336
12.5	2.717	2.071	2.706	0.844	0.747	0.812	31.688	27.514	33.496	22.014	20.650	22.269
20	3.661	2.774	3.650	1.440	1.247	1.388	41.196	35.580	43.682	32.327	29.968	32.862
25	4.217	3.186	4.208	1.848	1.583	1.785	46.649	40.185	49.541	38.729	35.688	39.477
50	6.541	4.892	6.541	3.947	3.253	3.845	68.553	58.556	73.180	67.326	60.815	69.328
75	8.452	6.282	8.464	6.077	4.884	5.957	85.794	72.898	91.883	92.411	82.479	95.840
100	10.137	7.498	10.162	8.204	6.473	8.082	100.556	85.113	107.956	115.287	102.036	120.230
125	11.670	8.600	11.709	10.316	8.022	10.204	113.708	95.951	122.316	136.557	120.100	143.063
150	13.092	9.618	13.147	12.407	9.533	12.315	125.703	105.802	135.442	156.572	137.017	164.669

H: Horizontal polarization; V: Vertical polarization; α: Angle of incidence; MP: Marshall and Palmer; RR: Rain rate in mm h^{-1}

Table 3: Specific attenuation and specific phase shift of vertically and horizontally polarized wave at frequency of 19.3 GHz for 1 km propagation path based on tropical lognormal drop size distribution and comparison with Marshall and palmer.

	Specific attenuation (dB km^{-1})						Specific phase shift (Deg km^{-1})					
	India			MP			India			MP		
	$\alpha = 90°$			$\alpha = 90°$			$\alpha = 90°$			$\alpha = 90°$		
RR	H	V	$\alpha = 0°$	H	V	$\alpha = 0°$	H	V	$\alpha = 0°$	H	V	$\alpha = 0°$
0.25	0.307	0.244	0.309	0.014	0.013	0.013	3.918	3.741	4.068	0.969	0.957	0.969
1.25	0.848	0.664	0.857	0.088	0.083	0.086	9.636	9.193	10.075	3.834	3.740	3.840
2.50	1.313	1.020	1.329	0.198	0.184	0.192	14.164	13.516	14.862	6.866	6.649	6.892
5.00	2.031	1.566	2.060	0.440	0.401	0.428	20.786	19.846	21.895	12.215	11.736	12.303
12.50	3.611	2.752	3.674	1.236	1.085	1.208	34.407	32.900	36.452	25.802	24.578	26.177
20.00	4.848	3.672	4.942	2.072	1.778	2.033	44.490	42.590	47.287	37.569	35.688	38.312
25.00	5.576	4.210	5.688	2.638	2.237	2.596	50.243	48.130	53.490	44.804	42.530	45.818

Table 3: Continued

	Specific attenuation (dB km^{-1})						Specific phase shift (Deg km^{-1})					
	India			MP			India			MP		
	$\alpha = 90°$			$\alpha = 90°$			$\alpha = 90°$			$\alpha = 90°$		
RR	H	V	$\alpha = 0°$	H	V	$\alpha = 0°$	H	V	$\alpha = 0°$	H	V	$\alpha = 0°$
50.00	8.602	6.429	8.800	5.503	4.490	5.469	73.182	70.283	78.333	76.587	72.723	79.124
75.00	11.082	8.229	11.357	8.356	6.659	8.363	91.073	87.633	97.819	103.877	98.842	108.066
100.00	13.261	9.801	13.608	11.168	8.755	11.238	106.295	102.441	114.463	128.372	122.430	134.259
125.00	15.240	11.221	15.657	13.931	10.784	14.081	119.790	115.603	129.263	150.859	144.198	158.459
150.00	17.074	12.531	17.557	16.644	12.756	16.885	132.046	127.584	142.739	171.796	164.556	181.108

H: Horizontal polarization; V: Vertical polarization; α: Angle of incidence; MP: Marshall and Palmer; RR: Rain rate (mm h^{-1})

Table 4: Specific attenuation and specific phase shift of vertically and horizontally polarized wave at frequency of 34.8 GHz for 1 km propagation path based on tropical lognormal drop size distribution and comparison with Marshall and palmer

	Specific attenuation (dB km^{-1})						Specific phase shift (Deg km^{-1})					
	India			MP			India			MP		
	$\alpha = 90°$			$\alpha = 90°$			$\alpha = 90°$			$\alpha = 90°$		
RR	H	V	$\alpha = 0°$	H	V	$\alpha = 0°$	H	V	$\alpha = 0°$	H	V	$\alpha = 0°$
0.25	0.697	0.600	0.716	0.054	0.053	0.054	4.797	4.765	4.941	1.742	1.722	1.744
1.25	1.836	1.567	1.894	0.326	0.307	0.324	10.968	10.983	11.361	6.625	6.485	6.658
2.50	2.778	2.361	2.871	0.693	0.642	0.691	15.546	15.643	16.148	11.485	11.197	11.574
5.00	4.194	3.550	4.344	1.441	1.313	1.442	21.915	22.185	22.834	19.537	18.997	19.763
12.50	7.203	6.061	7.484	3.640	3.242	3.671	34.167	34.942	35.766	38.063	37.026	38.744
20.00	9.487	7.958	9.875	5.735	5.052	5.810	42.694	43.947	44.812	52.640	51.344	53.779
25.00	10.807	9.052	11.260	7.078	6.204	7.189	47.395	48.954	49.813	61.121	59.737	62.559
50.00	16.166	13.476	16.892	13.321	11.502	13.636	65.172	68.156	68.806	95.335	94.100	98.172
75.00	20.426	16.979	21.384	18.990	16.264	19.534	78.162	82.452	82.759	121.933	121.395	126.033
100.00	24.096	19.989	25.260	24.257	20.660	25.039	88.720	94.238	94.144	144.276	144.727	149.537
125.00	27.378	22.674	28.732	29.214	24.780	30.238	97.747	104.434	103.908	163.796	165.414	170.137
150.00	30.379	25.126	31.911	33.922	28.680	35.188	105.703	113.512	112.534	181.263	184.169	188.620

H: Horizontal polarization; V: Vertical polarization; α: Angle of incidence; MP: Marshall and Palmer; RR: Rain rate (mm h^{-1})

way. Calculations of scattering impairments by rain in the tropical climates are therefore crucial since high rain rate are experienced in this region. The results presented also show that specific attenuation and specific phase shift are very dependence on the polarization. Radio signals experience more attenuation and absorption in the horizontal than in the vertical polarization. The difference between specific attenuation and specific phase shift based on Oblate spheroidal and spherical rain models are presented in Fig. 1 and 2, respectively. The difference in the specific attenuation increases with the rain rate at all the frequencies considered. It also increases with frequency for a fixed rain rate. Interestingly, the difference in phase shift at 16 and 19.3 becomes very large as the rain rate increase whereas the corresponding value at 34.8 GHz is within a very small range of angles throughout all the rain rates considered. This implies that spherical rain model has the tendency to underestimate rain-induced impairments when assumed in the propagation prediction on tropical path.

Figure 3 shows that the differential attenuation in both polarizations at all the frequencies considered and become very large as the rain rate increase; however it decreases with increase in frequency for a fixed rain rate. These are very important in the estimation of crosstalk in the design of radio communication systems, which is outside the scope of this work. Comparing the Indian data with those of Marshall and Palmer (1948) shows that their difference is not serious but comparatively higher at rain rates between 0.25 and 25 mm h^{-1} within 2.9 dB km^{-1} for specific attenuation and

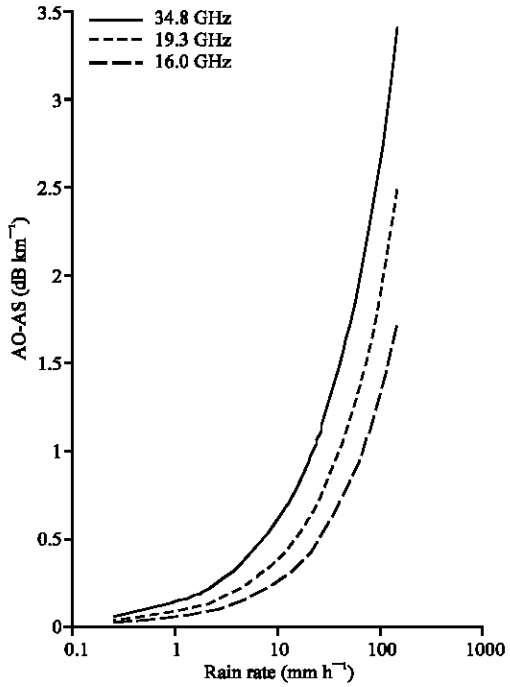

Fig. 1: Difference between the specific attenuation obtained from Oblate spheroidal and spherical rain models as a function of the rain rate based on the India drop size distribution at angle of incidence of 0°

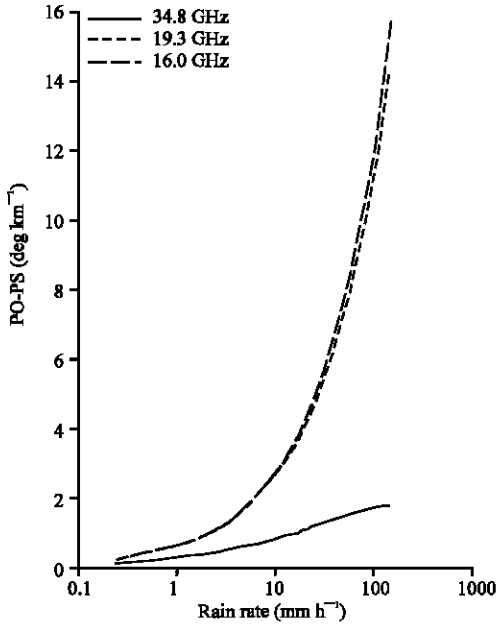

Fig. 2: Difference between the specific phase shifts obtained from Oblate spheroidal and spherical rain models as a function of the rain rate based on the India drop size distribution at angle of incidence of 0°

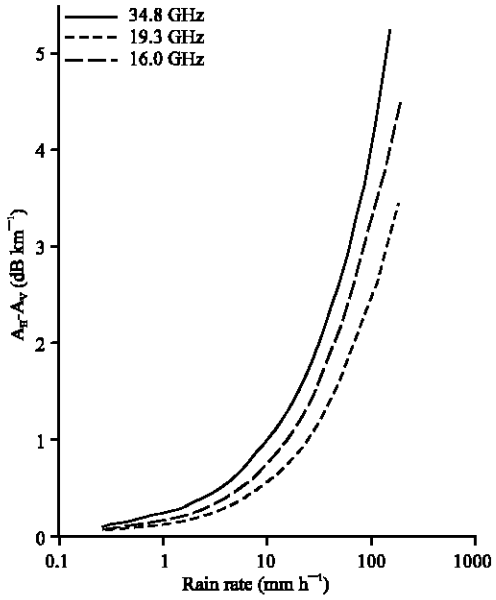

Fig. 3: Differential attenuation ($\Delta A = A_H - A_V$) obtained using Oblate spheroidal rain model as a function of the rain rate based on the Indian drop size distribution

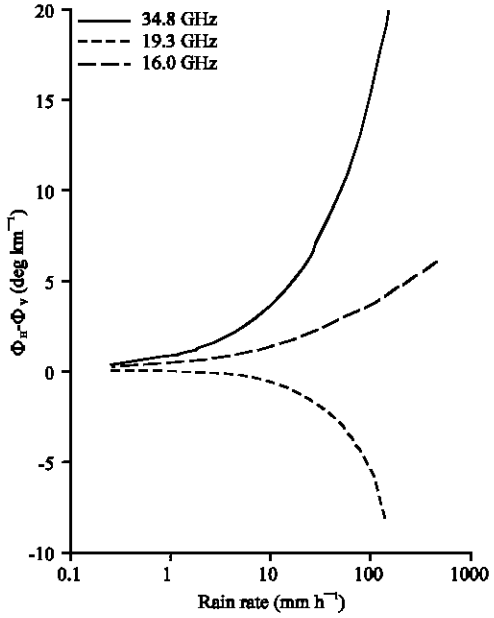

Fig. 4: Differential phase shift ($\Delta\Phi = \Phi_H - \Phi_V$) obtained using Oblate spheroidal rain model as a function of the rain rate based on the Indian drop size distribution

10 deg km^{-1} for specific phase shift. Note that the phase rotation at rain rate of 150 mm h^{-1} for instance is greater at frequency of 19.3 GHz than at frequency of 16 GHz whereas it reduces at frequency of 34.8 GHz. This is an indication that there is a peak frequency at which highest amount

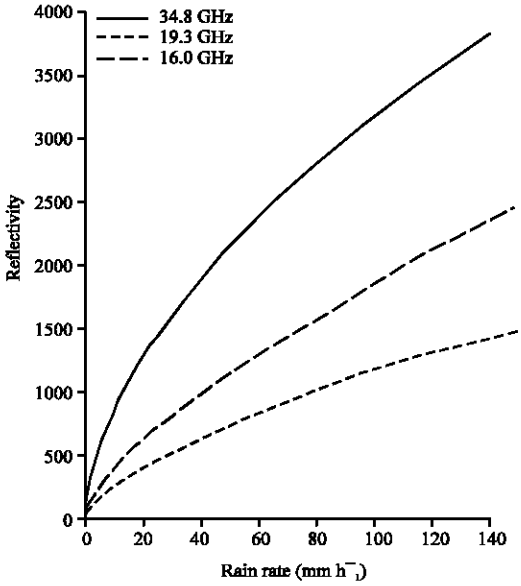

Fig. 5: Reflectivities obtained from spherical rain model as a function of the rain rate based on the Indian drop size distribution

Table 5: Power law relationship between Radar Reflectivity (η) and Rain rate obtained using the lognormal drop size distribution for spherical rain model and its comparison with those of Marshall and Palmer with oblate spheroidal rain model

F		India	MP[2]	MP[3]	J-D[2]	J-T[2]
16	a	50.170	-	-	-	-
	b	0.675				
19.3	a	81.050	-	-	-	-
	b	0.664				
34.8	a	205.380	-	-	-	-
	b	0.588				
94	a	167.000	135.00	139.00	110.00	69.00
	b	0.435	0.63	0.67	1.00	0.54
140	a	96.160	125.00	127.00	144.00	53.00
	b	0.479	0.55	0.60	0.79	0.51

F: Frequency GHz; [2]Aydin and Lure for side incidence; [3]Aydin and Lure for vertical incidence; The results are at horizontal polarization using Marshall and Palmer (MP), Joss Drizzle (J-D) and Joss Thunderstorm (J-T) drop size distribution

of phase rotation is experienced by radio signal as it is transmitted through the rain medium at 25 GHz for the Indian region. The differential phase shift as a function of rain rate is shown in Fig. 4. It also increase with the rain rate, however it decreases with frequency for a fixed value of rain rate. An exception to this result occurs for 34.8 GHz where the difference decreases rapidly to negative values.

The reflectivity generally increases with rain rate at all the frequency (Fig. 5). Empirical scaling relationship can be employed to estimate radar reflectivity for practical engineering application. The results obtained are used to obtain the parameters of the empirical approximation and this is shown in Table 5. Aydin and Lure (1991) earlier reported results of their computation at 94 and 140 GHz using Marshall and Palmer, Joss drizzle and Joss thunderstorm drop size distribution. The present result is therefore compared with those of Aydin and Lure (1991) at 94 and 140 GHz frequencies, though our computations are for spherical rain model but result for horizontal polarization of Oblate spheroidal rain model are reported by Aydin and Lure (1991), still, they compare well with those of Marshall and Palmer at 94 GHz.

CONCLUSIONS

In this study, scattering parameters of spherical and oblate spheroidal rain models are calculated using the Indian loguormal DSD and compared with MP DSD. Though MP DSD could underestimate specific attenuation and overestimate specific phase shift at some rain rates, however the Indian data still compared well at some other rain rate. The degree of suitability of assuming spherical rain model for rain-induced impairments prediction in tropical environment are reported. It was observed that spherical rain model could underestimate rain-induced impairments in a tropical path. The dependence of specific attenuation and specific phase shift on polarization are also investigated. Radio sigual suffers more attenuation and phase rotation in the horizontal than in the vertical polarization. The coefficients of the power law relationship between the radar reflectivity and rain rate reported in this paper agree well with those of Aydin and Lure (1991).

REFERENCES

Adekola, A.S., 2002. Millimeter radiowave scattering by tropical rain types. M. Tech. Thesis (unpublished).

Ajayi, G.O. and B.C. Ofoche, 1984. Some tropical rate characteristics at Ile-Ife for microwave and millimeter wave applications. J. Climate Applied Meteorol., 23: 562-567.

Ajewole, M.O., L.B. Kolawole and G.O. Ajayi, 1999. Theoretical study of effect of different types of tropical rainfall on microwave and millimeter-wave propagation. Radio Sci., 34: 1103-1124.

Aydin, K. and Y. Lure, 1991. Millimeter wave scattering and propagation in rain: A computational study at 94 and 140 GHz for oblate spheroidal and spherical raindrops. IEEE Trans. Geosci. Remote Sen., 29: 593-601.

Kunhikrishnan, P.K., R. Sivaraman and D.P. Alappattu, 2006. A case study of rain drop size distribution over a tropical Indian station. 36th COSPAR Scientific Assembly. Held 16-23 July, in Beijing, China, pp: 342.

Marshall, J.S. and W.M.K. Palmer, 1948. The distribution of raindrops with size. J. Meteorol., 5: 165-166.

Oguchi, T., 1966. Scattering and absorption of a millimeter wave due to rain and melting hailstones. J. Radio Res. Labortries, 13: 141-172.

Oguchi, T., 1980. Effect of incoherent scattering on attenuation and cross-polarization of millimeter-waves due to rain: Preliminary calculations at the 34.8 and 82 GHz for spherical raindrops. Ann. Telecommun., 35: 380-389.

Oguchi, T., 1981. Summary of studies on scattering of centimeter and millimeter waves due to rain and hail. Ann. Telecommun., 36: 383-399.

Oguchi, T., 1983. Electromaguetic wave propagation and scattering in rain and other hydrometeors. Proc. IEEE, 71: 1029-1078.

Oguchi, T., 1986. Effect of incoherent scattering on attenuation and depolarization of millimeter and optical waves due to hydrometeors. Radio Sci., 21: 717-730.

Oguchi, T., 1991. Effect of incoherent scattering on microwave and millimeter wave communications through rain. Electron Lett., 27: 759-760.

Ray, P.S., 1972. Broadband complex refractive indices of ice and water. Applied Optics, 11: 1836-1844.

Verma, A.K. and K.K. Jha, 1996. Rain drop size distribution model for Indian climate. Ind. J. Radio Space Phys., 25: 15-21.